Supplementary information

Reactivation of chromia poisoned oxygen exchange kinetics in mixed conducting solid oxide fuel cell electrodes by serial infiltration of lithia

Han Gil Seo[1+], Anna Staerz[1+], Dennis S. Kim[1,] Dino Klotz[1,2], Clement Nicollet[3], Michael Xu[1], James M. LeBeau[1], and Harry L. Tuller*[1]

[1]*Department of Materials Science and Engineering, Massachusetts Institute of Technology, Cambridge, MA, 02139, USA*

[2]*International Institute for Carbon-Neutral Energy Research (I²CNER), Kyushu University, Fukuoka, 819-0385, Japan.*

[3]*Université de Nantes, CNRS, Institut des Matériaux Jean Rouxel, IMN, F-44000 Nantes, France*

[+]*These authors contributed equally.*

[*]*Correspondence: tuller@mit.edu*

Experimental

Preparation of porous PCO specimen

The $Pr_{0.1}Ce_{0.9}O_{2-\delta}$ powder was synthesized by solution combustion route, starting from $Ce(NO_3)_3 \cdot 6H_2O$ (99.99%, Alfa Aesar), $Pr(NO_3)_3 \cdot 6H_2O$ (99.99%, Alfa Aesar) precursors and citric acid. The solution was heated on a hot plate and following gel combustion, the reaction resulted in the formation of a reddish powder. The resulting PCO powders were calcined at 750°C, 6 h in ambient air to blow away remaining organic species. The calcined powders were lightly pressed into a rectangular green body at approximately 70 MPa to make a porous specimen and then sintered at 1,450 °C for 3 h to produce a homogeneous grain size. The resulting PCO porous specimen ($20.7 \times 6.9 \times 0.9$ mm^3) was used for electrical conductivity relaxation measurements.

Electrical conductivity relaxation measurements

For the measurement of PCO conductivity, four gold wires were wound around the PCO specimen with gold paste painted along the wires to obtain better electrical contact. The electrical conductivity transients were performed with a HP3478A digital multimeter in a four-wire resistance measurement mode. The measurements were conducted in an alumina tube at temperatures (275 – 600°C, depending on infiltrants) with the P_{O_2} step between 0.1 and 0.2 atm controlled by two mass-flow controllers that mixed ultrahigh purity nitrogen and oxygen (grade 5.0, Airgas). Cr and Li nitrate-based solutions were prepared for infiltration, respectively, in ethanol to concentrations of 0.002 M (for 0.02 at%) and 0.2 M (more than 0.1 at%) for low and high loading. The pristine PCO specimen without any infiltration was first measured to extract the initial k_{chem} value. Following subsequent infiltration with the Cr-based nitrate solutions, measurements were repeated 3 times until the Cr concentration reached 0.3 at%. This final Cr infiltrated specimen was then serially infiltrated with Li_2O four more times ranging from 0.02 at% to 0.5 at%. The infiltration was performed while the sample was left hanging by its measurement wires so that the entire volume of solution remained inside the porous sample without dripping elsewhere, thereby increasing the precision and repeatability of the infiltration loading. After each infiltration, the specimen was calcined in situ under synthetic air at 600°C and measurements initiated when stabilization of the conductivity was achieved.

Microscopy analysis

The microstructures of pristine and serially infiltrated porous PCO specimen were examined by Zeiss Merlin High-Resolution scanning electron microscopy. The structure and chemical information were observed with a probe-corrected ThermoFisher Scientific Themis Z G3 60-300 kV S/TEM operated at

60 kV with a Gatan Continuum electron energy loss spectrometer (EELS). The electron probe current was approximately 25 pA with a probe convergence semi-angle of 30 mrad. The annular dark field imaging inner and outer detector collection semi-angles were 25 and 153 mrad respectively. All samples were prepared by diamond scribing the infiltrated PCO directly onto carbon film on 200 mesh copper transmission electron microscopy (TEM) grids (Ted Pella, Redding, CA). EELS chemical mapping was determined from multiple linear least squares (MLLS) fitting routine using the Gatan Microscopy Suite (GMS) software. The reference spectra for Cr and Ce/Pr were taken from regions in the Cr_2O_3-**only** infiltrated PCO (0.3 at%). The spectra around the O-K edge and $Cr-M_{2,3}$ edge corroborate the low-loss reference spectra corresponds to the Cr rich regions. Reference spectra for Li were taken from regions in Li-**only** infiltrated PCO (0.3 at%). The reference spectra for Li-K edge is shown as the yellow line in Figure 2h along with the spectra in regenerated Li-infiltrated PCO around the Li-K and $Cr-M_{4,5}$ edge (left) and O-K and $Cr-L_{2,3}$ edge (right). The reference spectra for Li-K edge was determined from a Li-only infiltrated PCO. The decrease in elemental intensity towards the bulk of the PCO is due to plural inelastic scattering with material thickness.

Fabrication of symmetric cells

Symmetric cells with PCO/YSZ/PCO configuration were fabricated to measure the area-specific resistance. 70 µl of 1,5-pentanediol (AlfaAesar, 97%) and 10 µl of an Optapix PAF 35/water (50:50, Zschimmer & Schwarz Inc.) were added to 0.2 g of the PCO powder and ground into a paste using a mortar and pestle. The PCO slurry was screen printed onto one side of a YSZ (100) single crystal substrate (MTI, doubly polished, $10x10x0.5$ mm^3) and dried for 4 h at room temperature and then overnight at 90°C. This process was repeated onto the second side of the YSZ. The sample was then sintered in a tubular furnace at 1350°C for 3 h under ambient air. Gold paste (fuelcellmaterials) was then applied to both sides of each of the prepared PCO electrodes as current collector. The pristine sample was used as is. After measuring the pristine cell, a 0.2 M ethanol solution of Cr-nitrate was used to infiltrate the cell with 0.15 at% Cr (based on an average weight of 0.012 g per electrode after screen printing and calcination). The cell was measured and again infiltrated with 0.4 at% Li using a 0.2 M ethanol solution of Li-nitrate.

Electrochemical measurements

Electrochemical analyses of symmetric cells with pristine and infiltrated PCO electrodes were conducted by electrochemical impedance spectroscopy measurements with a Solartron 1255 HF frequency response analyzer interfaced with an EG&G PAR potentiostat model 273A in the frequency range of 0.1 Hz to 1 MHz in the temperature range of 450 – 650ºC at an oxygen partial pressure between

0.1 and 0.5 atm. The cells were placed in an alumina tube and the gold current collector was connected to a platinum wire under gas mixtures of oxygen and nitrogen delivered through digital mass flow controllers. Distribution relaxation of time (DRT) analyses were carried out with DRTtools[1,2] in order to investigate the characteristic process in more detail. The area under P1 was determined using the integrate function of the Peak Analyzer Tool in Origin2020b. The normalization factor was determined by the total area of all peaks to the resistance of the total ASR of the Nyquist plot for the pristine cell at 575 °C. This auxiliary equivalent circuit consisted of a series resistance accounting for all higher frequency processes and a resistor in parallel with a constant phase element, which is often referred to as R-Q circuit. The following mathematical representation of the R-Q circuit was chosen in order to directly obtain τ and R:

$$Z_{RQ}(\omega) = \frac{R}{1 + (j\omega\tau)^{\alpha}}$$

The chemical capacitance was obtained by normalizing the values to the volume of the cell (determined using the weight of the PCO layer and its density).

Supplementary Note 1: Electrical conductivity relaxation measurements: porous PCO specimen

1-1) Gas phase diffusion limit

In order to evaluate if gas phase diffusion within the pores in the porous specimen influences the determination of k_{chem}, we compared three different samples, $La_{0.6}Sr_{0.4}CoO_{3-\delta}$ (LSC) thin film (with sufficient high exchange kinetics), porous PCO specimens with different thickness and the response of the oxygen probe (YSZ tube with Pt electrode). Figure S1a presents the conductivity transient profiles measured at 600°C for which the oxygen exchange kinetics are much faster than the flush time of the experimental setup and the corresponding results are also compared with the flush time measured with an oxygen probe.
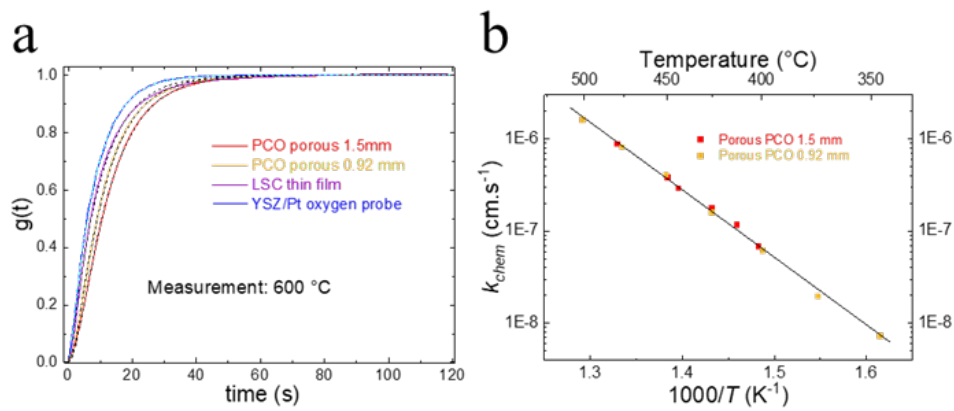
Figure S1. (a) Normalized conductivity relaxation profiles in response to pO_2 step (0.1 to 0.2 atm) for pristine PCO specimens with different thickness, LSC thin film and YSZ/Pt oxygen probe. (b) Oxygen surface exchange coefficients (k_{chem}) of PCO with different thickness as a function of temperature.

We use the flush time corrected relaxation expression from M. W. Den Otter *et al.*[3], which gives a flush time constant τ_f as well as a "reaction" time constant τ_n as follow:

$$g(t) = 1 - \exp\left(\frac{-t}{\tau_f}\right) - \frac{\tau_n}{\tau_n - \tau_f}\left(\exp\left(\frac{-t}{\tau_n}\right) - \exp\left(\frac{-t}{\tau_f}\right)\right)$$

Table S1. Flush time and reaction time constants of porous PCO specimens with different thickness, LSC thin film and oxygen probe.

Sample	Flush time constant (τ_f, sec)	Reaction time constant (τ_n, sec)
Oxygen probe	7.6	0.63
LSC thin film	9.2	0.71
Porous PCO (0.92 mm thickness)	9.3	2.3
Porous PCO (1.5 mm thickness)	9.9	3.2

Table S1 represents comparison of flush time and reaction time constants of different samples. The flush time constant for the oxygen probe is slightly lower than for any of the conductivity samples. This is attributed to the fact that the introduction of the probe into the setup reduces the reactor volume, which leads to a reduced flush time constant. Given that τ_n increases from that of the LSC thin film to that of the porous PCO specimen (1.5 mm thickness), this implies that gas phase diffusion within the pores impacts the measured transient, but only when the temperature is sufficiently high so that the oxygen exchange kinetics begin to drop below the flush time. Indeed, although the porous samples with different thicknesses yield slightly different profiles in the flush time limited regime, the k_{chem} values derived from the profiles measured at lower temperatures are identical (Figure S1b). We further observed that an additional set of porous PCO specimens achieved by utilizing different sintering temperatures (1350℃ and 1450℃), and therefore different levels of porosity, yield identical time constants (ca. 10 s), as presented in Figure S2. This agrees well with the values in Table S1.
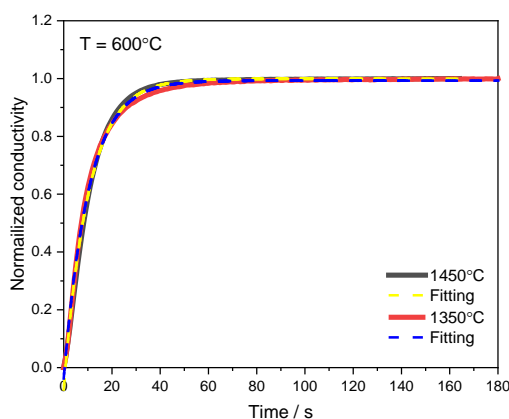

Figure S2. Normalized conductivity relaxation profiles in response to pO$_2$ step (0.1 to 0.2 atm) for the pristine PCO specimens sintered at 1450°C and 1350°C resulting in the same time constant (*10 s*).

Y. Zhang *et al.* argue about the importance of utilizing a distribution of time constants in analyzing kinetic data, particularly at higher measurement temperatures, when gas diffusion and gas exchange kinetic become comparable.[4] In our study, we chose to avoid those issues by measuring our samples in a much lower temperature range. Furthermore, given the flush time is independent of temperature, and gas diffusion is only weakly dependent on temperature[4], one can conclude that the measurement conditions used in this work are set so that the influence of gas diffusion is negligible.

1-2)   Bulk oxygen diffusion and surface oxygen exchange kinetics limits

Ignoring gas phase diffusion contributions, the overall relaxation profiles can be readily affected by both bulk oxygen diffusion through the sample and surface oxygen exchange kinetics on the surface. To determine which of the two limits the overall relaxation process, the critical thickness (above which oxygen ion transport through the electrode becomes dominant) has to be considered, which follows as: $L_c = {D}/{k}$ where D and k are the oxygen diffusion and oxygen exchange coefficients, respectively. The porous specimen prepared in this work has an approximately 1-µm grain size, which is advantageous given the much shorter oxygen ion diffusion length than the critical thickness (3.6×10^3 mm at 670°C)[5]. In addition, based on the literature[3], it turns out that $L_\alpha = a/L_c = a * {k}/{D} < 0.03$, the surface exchange-controlled kinetic becomes dominant, but if $L_\alpha > 30$, oxygen diffusion-controlled kinetics becomes dominant. The calculated value of L_α in this case is less than $0.0003 \ll 0.03$, clearly indicating surface exchange-controlled kinetics. One concludes that the overall relaxation process under measurement conditions is limited not by oxygen ion diffusion through the sample but by surface oxygen exchange kinetics.
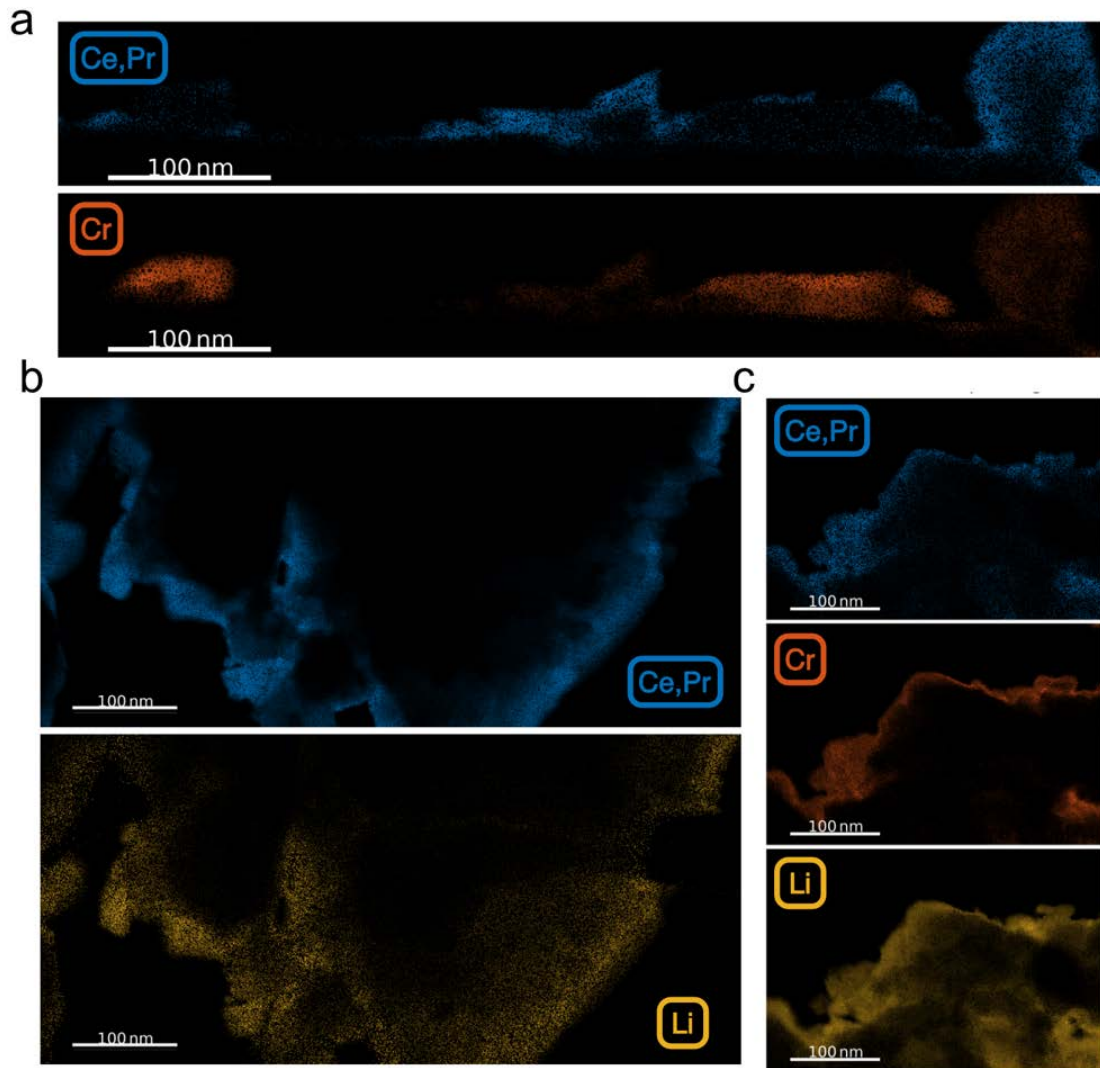
Figure S3. Electron Energy Loss Spectroscopy (EELS) elemental mapping of (**a**) Ce(Pr)-$N_{4,5}$ edge and Cr-$M_{2,3}$ and in Cr_2O_3-infiltrated PCO. (b) Elemental mapping of Ce(Pr)-$N_{4,5}$, and Li-K edge in Li_2O-infiltrated PCO. (**c**) Elemental mapping of Cr-$M_{2,3}$ edge in serial infiltrated PCO.

Supplementary Note 2: Profile fitting in pristine, Cr- and serially Cr-/Li-infiltrated PCO specimen

1-1)   Introduction of fitting procedure

Electrical conductivity relaxation measurements can be used to examine bulk oxygen diffusion (D_{chem}) and surface oxygen exchange kinetics (k_{chem}). The electrical conductivity of mixed conducting oxides depends on their oxygen stoichiometry driven by the oxygen activity (i.e. oxygen partial pressure) in the surrounding gas. By monitoring the transient in electrical conductivity through a rapid change in surrounding oxygen partial pressure, one can analyze the characteristics of the kinetics associated with the uptake or release of oxygen from the oxide. As already noted in Supplementary Note 1, in this case, the overall exchange kinetics of a porous PCO specimen used in this work is limited by the surface oxygen exchange kinetics, which can be simply expressed by[6]:

$$\bar{C}(t) = \frac{C(t)-C_0}{C_\infty - C_0} = 1 - \exp(-k_{chem}\frac{A}{V}t) \qquad \text{Equation 1}$$

where $C(t)$, C_0, and C_∞ are the concentration of oxygen in the oxide at time t, at the initiation of the step in pO_2 and at infinite time, respectively. The geometrical factor A/V corresponds to the surface area to volume ratio of the PCO. The volume V is related to the fraction of porosity p subtracted from the overall geometric volume V_{total} of PCO, expressed by $V=V_{total}(1-p)$. The porosity p of the PCO specimen is 0.26. The surface area per volume ($S_A=A/V_{total}$) was determined by SEM cross-sectional imaging, with a line intersection analysis according to stereology theory.[7] The value of S_A (26,500 cm^2·cm^{-3}) was used.[6] Since the change in concentration of oxygen in the oxide leads to the change in electrical conductivity, Equation 1 can be converted to Equation 2 as follows:

$$g(t) = \frac{\sigma(t)-\sigma_0}{\sigma_\infty - \sigma_0} 1 - \exp\left(-k_{chem}\frac{A}{V}t\right) = 1 - \exp\left(-\frac{t}{\tau}\right) \qquad \text{Equation 2}$$

where $\sigma(t)$, σ_0, and σ_∞ are the electrical conductivity at time t, and τ is the time constant of the transient. The oxygen exchange coefficient (k_{chem}) can be calculated by using Equation 3:

$$k_{chem} = \frac{V}{A\cdot\tau} = \frac{(1-p)}{S_A\cdot\tau} \qquad \text{Equation 3}$$

1-2)   Cr-infiltrated specimen

The influence of Cr poisoning on the relaxation profiles was studied in a preliminary work considering much lower Cr loading below 0.02 at%. In that case, two time constants were necessary to fit the data accurately. It was observed that as the Cr loading amount increases, the A_1 (pristine PCO-rich) fraction decreases while the A_2 (Cr-rich) fraction increases, as shown in Figure S4. On the other hand, the relaxation profile of Cr-infiltrated PCO specimen (from 0.02 at % to 0.3 at%) could be fitted very well by the single time constant exponential equation. One should keep in mind, that once Cr-species are infiltrated into PCO, the transient rates become much slower than the pristine PCO (factor > 20). This is expected for either a dramatically decreased active surface area or much slower kinetics in the region affected by Cr; or both. Observing only one time constant in the relaxation profile at higher Cr-species concentrations can have several reasons: (1) the pristine PCO region becomes negligibly small, (2) the Cr-infiltrated region has negligible oxygen exchange. We can extrapolate that A_1 eventually reaches 0 and the profiles return to a one time constant shape, in line with what is observed in the manuscript (Cr-infiltration level above 0.02 at%). For these reasons, we chose a single time constant exponential equation to fit the Cr-infiltrated (above 0.02 at% in this work) sample instead of using two time constant exponentials, as presented in Figure S5b-d.
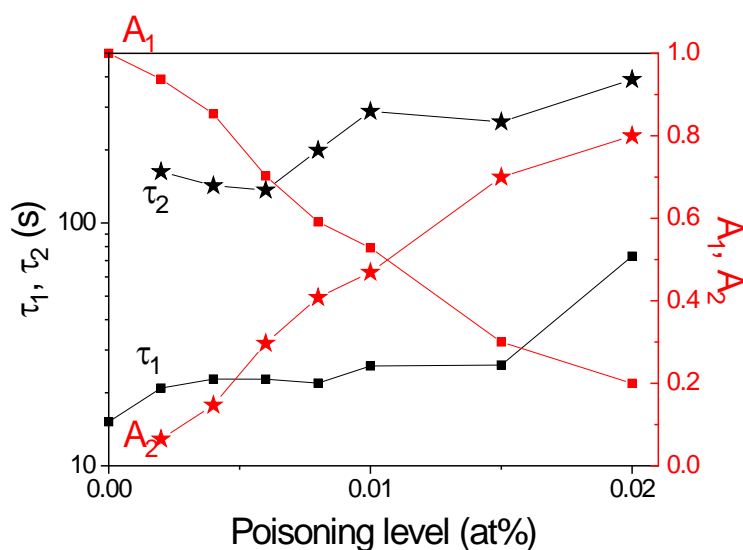

Figure S4. Evolution of the fitting parameters as a function of Cr loading level below 0.02 at%.

1-3)   Cr-/Li-infiltrated specimen

As can be seen in Figure S5, while the relaxation profiles of the pristine, Cr-infiltrated and subsequently 0.02 at % Li-infiltrated PCO fit a single time constant (τ) exponential well (green dashed line in Figure S5a-e), those of serially Li-infiltrated PCO with high concentrations (up to 0.5 at%) are fit well with two time constant (τ_1 and τ_2) exponentials (orange dashed line in Figure S5f-h). Along with observation of the Cr-infiltrated specimen, we attributed the changes in profiles with high concentrations of Li-infiltration to the presence of two distinguishable areas with faster (Li-rich) and slower (Cr-rich) kinetics, respectively. A_1 and A_2, corresponding to τ_1 and τ_2 in orange dashed expression (Figure S5f-h), are the fractional area for each time constant. Following serial Li-infiltration on a Cr-poisoned PCO surface, the detrimental effect of Cr_2O_3 crystallites on surface kinetics is expected to become less. A_1, A_2, τ_1 and τ_2 values of subsequently Li-infiltrated PCO with high concentrations (0.1 at% to 0.5 at%, obtained by fitting the orange dashed equation, are summarized in Table S2. As expected, it shows that a continuous shift from the long to the short time constant, as one goes from more Cr-rich (τ_2) to Li-rich (τ_1) compositions. This is further consistent with the corresponding fractional change from large Cr-rich area (A_2) to large Li-rich area (A_1). Average time constant values at high concentrations of Li-infiltration, used in Figure 2b in the main text, were calculated by use of the following expression: $\tau_{average} = A_1 \cdot \tau_1 + A_2 \cdot \tau_2$.
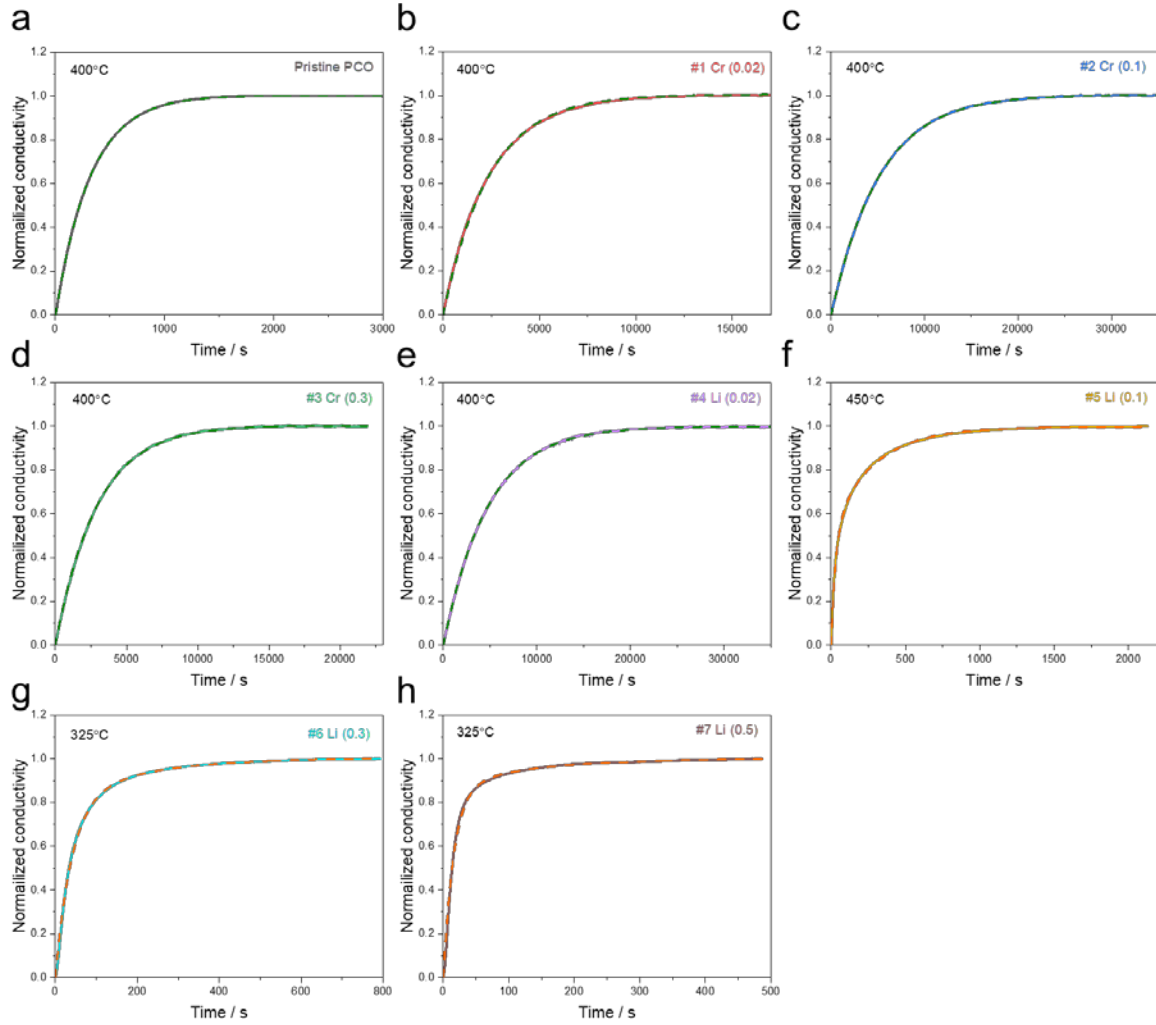
Figure S5. Normalized conductivity relaxation profiles in response to pO_2 step (0.1 to 0.2 atm) beginning with a pristine PCO specimen and following successive Cr- and Li-infiltration. **(a)** Pristine, **(b)** #1 Cr (0.02), **(c)** #2 Cr (0.1), **(d)** #3 Cr (0.3), **(e)** #4 Li (0.02), **(f)** #5 Li (0.1), **(g)** #6 Li (0.3) and **(h)** #7 Li (0.5). Unit in parentheses is at%. The profiles of **(a-e)** and **(f-h)** were fitted by the green (single time constant) and orange (two time constant) expressions, respectively.

Table S2. Fitting results of normalized conductivity relaxation transient, measured on PCO specimen with following successive Cr- and Li-infiltration at 325°C through two time constant exponential equation, as shown in Figures S5f-h.

| At 325°C	Li-rich		Cr-rich	
Samples	A_1	τ_1	A_2	τ_2
#5 Li (0.1 at%)	0.53[*]	32[*]	0.47[*]	284[*]
#6 Li (0.3 at%)	0.80	40	0.20	200
#7 Li (0.5 at%)	0.87	16	0.13	130

τ_1 and τ_2: time constant in seconds
A_1 and A_2: fraction for each time constant τ_1 and τ_2
*[*]These values were obtained at 450 ℃. (not measured at 325 ℃)*
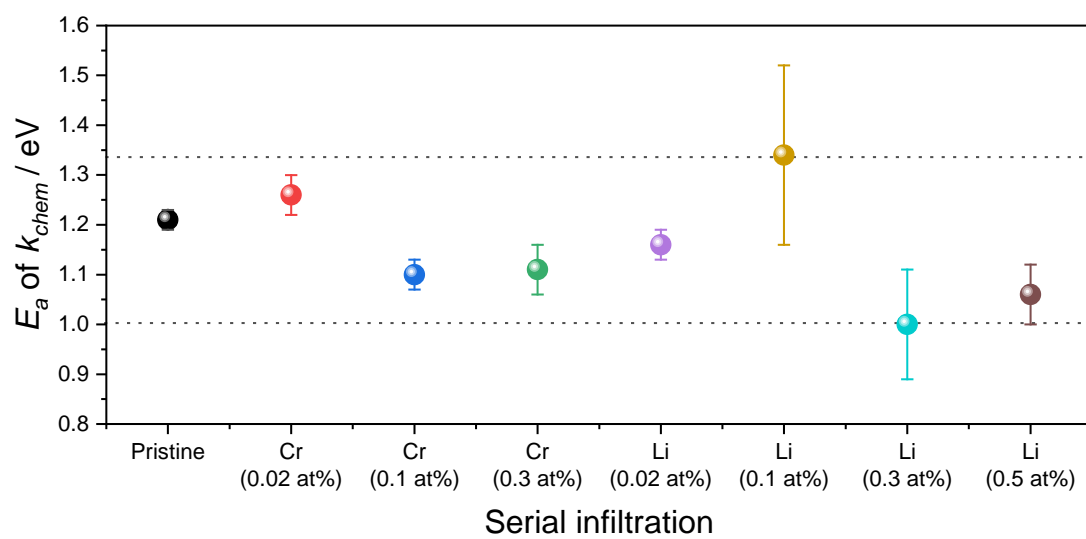
Figure S6. Activation energies (E_a) of k_{chem} of PCO porous specimen with serial infiltration using the Cr- and the Li-sources.
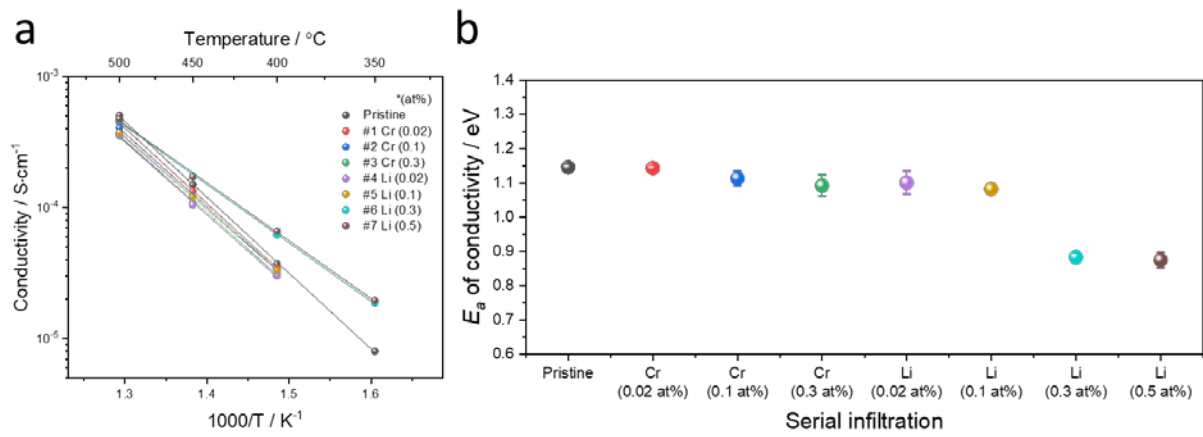
Figure S7. (**a**) The overall conductivity (σ) and (**b**) corresponding activation energies (E_a) of pristine PCO porous specimen with serial infiltration using Cr- and Li-sources.
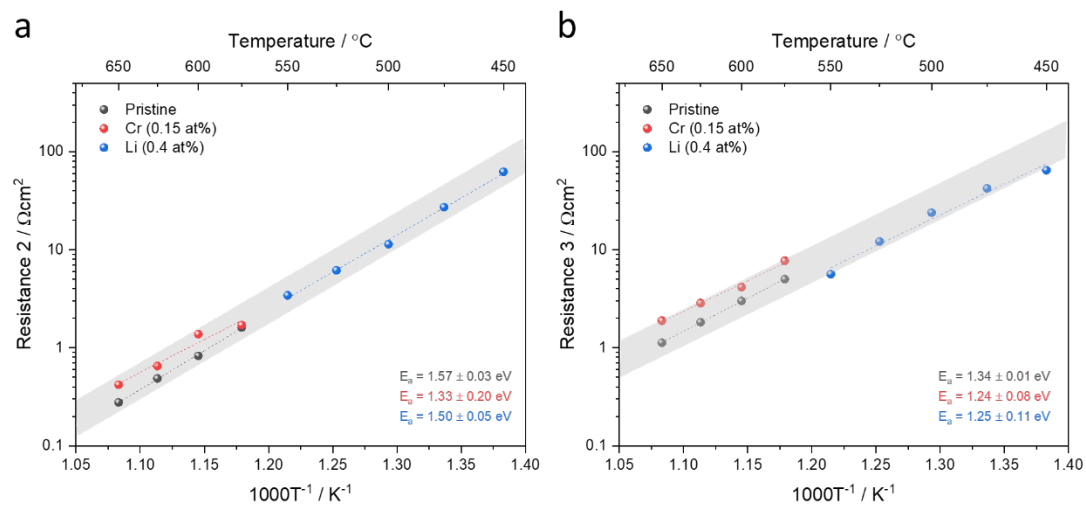
Figure S8. Temperature dependence of **(a)** resistance 2 (*R2*) and **(b)** 3 (*R3*) obtained from Nyquist plot of the pristine cell after Cr-infiltration and with subsequent Li-infiltration.
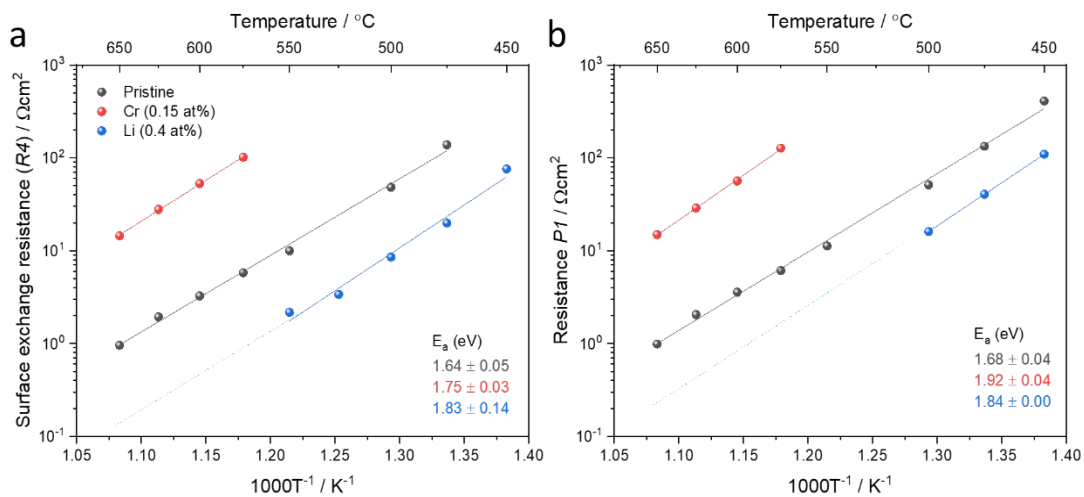
Figure S9. Temperature dependence of **(a)** surface exchange resistance (*R4*) and **(b)** resistance of *P1* of the pristine cell after Cr-infiltration and with subsequent Li-infiltration obtained from Nyquist plot and DRT, respectively.
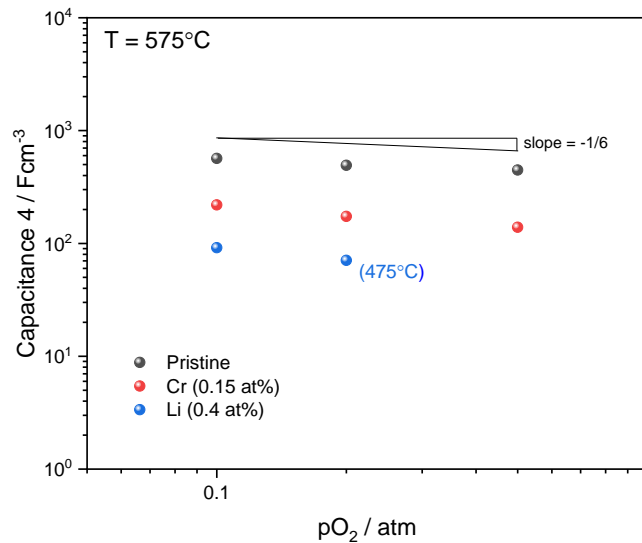
Figure S10. Oxygen dependence of capacitance 4 (*C4*) of the pristine cell after Cr-infiltration and with subsequent Li-infiltration obtained at 575°C. The data of Li-infiltration was extracted at 475°C due to the limit of fitting at high temperatures.

References

1. T. H. Wan, M. Saccoccio, C. Chen and F. Ciucci, *Electrochim. Acta*, 2015, **184**, 483–499.

2. F. Ciucci and C. Chen, *Electrochim. Acta*, 2015, **167**, 439–454.

3. M. W. den Otter, H. J. M. Bouwmeester, B. A. Boukamp and H. Verweij, *J. Electrochem. Soc.*, 2001, **148**, J1.

4. Y. Zhang, F. Yan, B. Hu, C. Xia and M. Yan, *J. Mater. Chem. A*, 2020, **8**, 17442–17448.

5. D. Chen, S. R. Bishop and H. L. Tuller, *J. Electroceramics*, 2012, **28**, 62–69.

6. C. Nicollet, C. Toparli, G. F. Harrington, T. Defferriere, B. Yildiz and H. L. Tuller, *Nat. Catal.*, 2020, **3**, 913–920.

7. E. E. Underwood, eds. J. L. McCall and W. M. Mueller, Springer US, Boston, MA, 1973, 35–66.